ISSN: 0256-307X

中国物理快报

Chinese Physics Letters

Volume 32 Number 4 April 2015

A Series Journal of the Chinese Physical Society
Distributed by IOP Publishing

Online: http://iopscience.iop.org/0256-307X
http://cpl.iphy.ac.cn

CHINESE PHYSICAL SOCIETY
IOP Publishing

CHIN. PHYS. LETT. Vol. 32, No. 4 (2015) 045201

On the Gradient of the Electron Pressure in Anti-Parallel Magnetic Reconnection *

WANG Huan-Yu(王焕宇), HUANG Can(黄灿)**, LU Quan-Ming(陆全明), WANG Shui(王水)

CAS Key Laboratory of Geospace Environment, Department of Geophysics and Planetary Science, University of Science and Technology of China, Hefei 230026

(Received 22 October 2014)

We first perform a two-dimensional particle-in-cell simulation of anti-parallel magnetic reconnection to verify that in the electron diffusion region the reconnection electric field is mainly balanced by the gradient of the electron pressure. Then, by following typical electron trajectories in the fixed electromagnetic field of anti-parallel reconnection, we calculate the gradient of the electron pressure. We find that the resulted gradient of the electron pressure is equal to the reconnection electric field. This indicates that in the electron diffusion region the reconnection electric field is balanced by the gradient of the electron pressure, which results from the electron nongyrotropic motions. Our result gives a microphysical explanation of the balance between the reconnection electric field and the gradient of the electron pressure.

PACS: 52.20.Dq, 52.65.Rr DOI: 10.1088/0256-307X/32/4/045201

As a fundamental physical process in plasma, magnetic reconnection is closely related to the rapid energy conversion: the magnetic free energy stored in a current sheet suddenly releases, which accelerates and heats the plasma.[1–7] The diffusion region, which is strongly localized and extending several ion Larmor radius in collisionless reconnection,[8–11] facilitates the topological changes of the magnetic field lines.

Derived from the Vlasov equation, the electron momentum equation without classical collisions can be expressed as[11–14]

$$\boldsymbol{E} = -\boldsymbol{V}_e \times \boldsymbol{B} - \frac{1}{n_e e}\nabla \cdot \boldsymbol{P}_e - \frac{m_e}{e}\left(\frac{\partial \boldsymbol{V}_e}{\partial t} + \boldsymbol{V}_e \cdot \nabla \boldsymbol{V}_e\right), \quad (1)$$

where $\boldsymbol{E}$ and $\boldsymbol{B}$ are the electric field and the magnetic field, $\boldsymbol{P}_e$ is the electron pressure tensor, n_e and $\boldsymbol{V}_e$ are the electron density and bulk velocity. The right-hand side (RHS) of Eq. (1) is composed of three parts: the first term representing the electron convection effect, the second term showing the gradient effect of electron pressure, and the last term containing the inertial effect of the electrons. In the two-dimensional (2D) case, where magnetic reconnection is assumed to occur in the (x, z) plane with $\partial/\partial y$=0, the y component for Eq. (1) is

$$\begin{aligned} E_y = & -(V_{ez}B_x - V_{ex}B_z) \\ & - \frac{1}{n_e e}\left(\frac{\partial P_{exy}}{\partial x} + \frac{\partial P_{eyz}}{\partial z}\right) \\ & - \frac{m_e}{e}\left(\frac{\partial V_{ey}}{\partial t} + V_{ex}\frac{\partial V_{ey}}{\partial x} + V_{ez}\frac{\partial V_{ey}}{\partial z}\right). \end{aligned} \quad (2)$$

The characteristic lengths below which the electron convection, the gradient of the electron pressure, and the electron inertial terms take place are $c/\omega_{\rm pi}$, $c/\omega_{\rm pe}$ and $c/\omega_{\rm pe}$, respectively, (where $\omega_{\rm pi}$ and $\omega_{\rm pe}$ are the plasma frequencies for ions and electrons while $c/\omega_{\rm pi}$ and $c/\omega_{\rm pe}$ are the inertial lengths for ions and electrons). The vicinity of the X line in anti-parallel magnetic reconnection has multi-scale structures.[5,6,15–17] In the ion diffusion region (with the scale of the ion inertial length) the electrons are frozen in the magnetic field while ions are unmagnetized, which causes the Hall effect: a quadruple structure of the out-of-plane magnetic field and the reconnection electric field dominated by the electron convection. In the electron diffusion region (with the scale of the electron inertial length), both ions and electrons are unmagnetized, and the reconnection electric field is balanced mainly by the gradient of the electron pressure. The electron inertial term is considered to be negligible in both the ion and electron diffusion regions. It has recently been demonstrated that the evolution of the gradient of the electron pressure in the electron diffusion region is related to the onset of magnetic reconnection.[18]

Although it is generally accepted that the reconnection electric field in the vicinity of the X line during anti-parallel reconnection is balanced mainly by the gradient of the electron pressure, which is demonstrated by comparing the two terms obtained from 2D particle-in-cell (PIC) simulations,[7–10] the detailed microphysics is still unknown. In this Letter, by studying electron dynamics in the electron diffusion region, we demonstrate that the reconnection electric field is balanced by the gradient of the electron pressure, while the gradient of the electron pressure is generated due to the electron nongyrotropic motion.[19] This gives a microphysical explanation of the balance between the reconnection electric field and the gradient of the electron pressure in the electron diffusion region.

A 2D PIC simulation code is used here, which has been widely used to study magnetic

*Supported by the National Natural Science Foundation of China under Grant Nos 41331067, 11220101002, 11235009, 41274144 and 41121003, the National Basic Research Program of China under Grant Nos 2013CBA01503 and 2012CB825602, the Ph.D. Foundation of the Ministry of Education of China under Grant No 20123402120010, and the Knowledge Innovation Program of Chinese Academy of Sciences under Grant No KZZD-EW-01-4.

**Corresponding author. Email: canhuang@mail.ustc.edu.cn

reconnection.[20–22] The initial configuration is a 1D Harris current sheet in the (x, z) plane, where the initial magnetic field is given as

$$\boldsymbol{B}_0(z) = B_0 \tanh(z/\lambda)\boldsymbol{e}_x, \tag{3}$$

where B_0 is the asymptotical magnetic strength and λ is the half width of the current sheet. The corresponding number density is

$$n(z) = n_\mathrm{b} + n_0 \mathrm{sech}^2(z/\lambda), \tag{4}$$

where n_b is the number density of the background plasma, and n_0 is the peak Harris number density. The initial distribution functions for the ions and electrons are Maxwellian with a drift speed in the y direction satisfying $V_{\mathrm{i}0}/V_{\mathrm{e}0} = -T_{\mathrm{i}0}/T_{\mathrm{e}0}$, where $V_{\mathrm{i}0}$ ($V_{\mathrm{e}0}$) and $T_{\mathrm{i}0}$ ($T_{\mathrm{e}0}$) are the initial drift speed and temperature of ions (electrons), respectively. In the simulation, we set the temperature ratio as $T_{\mathrm{i}0}/T_{\mathrm{e}0} = 4$, and the density ratio is $n_\mathrm{b}/n_0 = 0.2$. The initial half width of Harris current sheet is $\lambda = 0.5c/\omega_{\mathrm{pi}}$, where c/ω_{pi} is defined by n_0. The mass ratio is m_i/m_e=100 and light speed is $c = 15V_\mathrm{A}$, where V_A is the Alfvén speed based on B_0 and n_0. The computation is carried out in a rectangular domain in the (x, z) plane whose size is $(12.8c/\omega_{\mathrm{pi}}) \times (6.4c/\omega_{\mathrm{pi}})$ with grid number 512×256. Thus, the spatial resolution is $0.025c/\omega_{\mathrm{pi}} = 0.25c/\omega_{\mathrm{pe}}$. The time step is $\Omega_\mathrm{i}\Delta t = 0.001$, where Ω_i is the ion gyro-frequency. We employ 10^9 particles in the simulation domain. The periodic boundary conditions are used along the x direction. The ideal conducting boundary conditions for the electromagnetic fields and reflected boundary conditions for particles are used in the z direction.

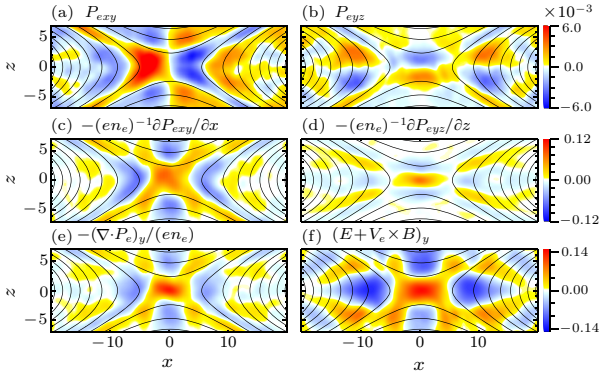

Fig. 1. The electrons off-diagonal pressure tensor terms P_{exy} (a) and P_{eyz} (b), the gradient of P_{exy} (c) and P_{eyz} (d), the sum of the two gradient terms (e), and the non-ideal electric field $(E+V_e\times B)_y$ (f) at $\Omega_\mathrm{i}t$=15 in the anti-parallel reconnection. The in-plane magnetic field lines are also presented.

A single X line is formed near the center of the simulation domain and the reconnection rate attains its maximum around $\Omega_\mathrm{i}t = 16$. Figure 1 exhibits the electron off-diagonal pressure tensor terms P_{exy} (Fig. 1(a)) and P_{eyz} (Fig. 1(b)), the gradient of P_{exy} (Fig. 1(c)) and P_{eyz} (Fig. 1(d)), the sum of the two gradient terms (Fig. 1(e)), and the non-ideal electric field $(\boldsymbol{E} + \boldsymbol{V}_e \times \boldsymbol{B})_y$ at $\Omega_\mathrm{i}t = 16$ (Fig. 1(f)). The off-diagonal term P_{exy} has a bipolar structure along $z = 0$ around the X line, while the off-diagonal term P_{eyz} has a bipolar structure along $x = 0$ around the X line. Their gradients peak at the X line. From Figs. 1(e) and 1(f), we can also find that the non-ideal electric field $\boldsymbol{E}+\boldsymbol{V}_e\times\boldsymbol{B}$ around the X line is well represented with the gradient of electron pressure term near the X line (the electron diffusion region with the size around c/ω_{pe}), which implies that the electron inertial effect is significantly small there.[15,18] This can be seen more clearly in Fig. 2, which shows the profile of the reconnection electric field, the electromotive force term, and the off-diagonal electron pressure tensor term along $z = 0$ at $\Omega_\mathrm{i}t = 16$. The electromotive force term supports the reconnection electric field at $|x| \geq 0.3c/\omega_{\mathrm{pi}}$. In the vicinity of the X line with $|x| \leq 0.3c/\omega_{\mathrm{pi}}$, the reconnection electric field is mainly balanced by the off-diagonal electron pressure tensor term. Note that the spatial coordinates in the figures are normalized by the electron inertial length.

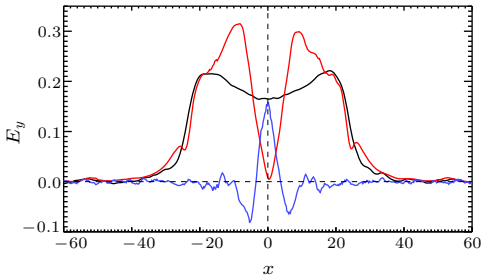

Fig. 2. Profiles of the reconnection electric field (the black line), the electromotive force term (red line) and the off-diagonal electron pressure tensor term (blue line) along $z = 0$ at $\Omega_\mathrm{i}t = 16.0$.

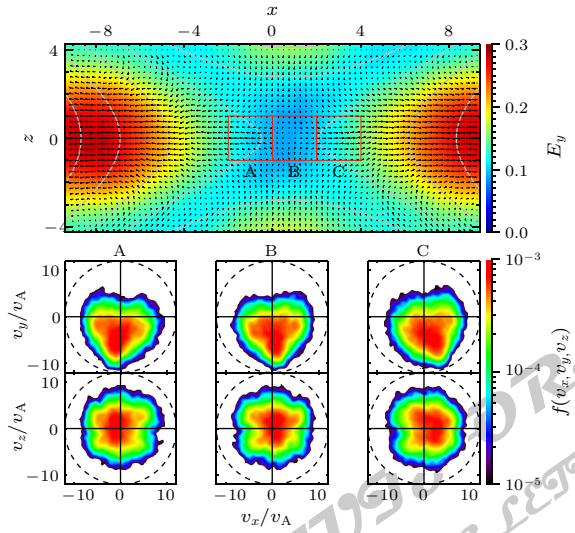

Fig. 3. The in-plane electron flow vectors in the anti-parallel reconnection and the out-of-plane electric field (filled contours) are shown in the top panel. The bottom panel shows the electrons velocity distributions $f(v_x, v_y)$ and $f(v_x, v_z)$ in the marked regions in the top panel.

Figure 3 shows the in-plane electron bulk flow vectors (the arrows in the top panel) and the corre-

sponding electron velocity distributions $f(v_x, v_y)$ and $f(v_x, v_z)$ (the bottom panel) in three different regions (marked with A, B and C, respectively) around the X line at $\Omega_i t = 16$. The background colors and solid lines in the top panel represent the out-of-plane electric field and in-plane magnetic field lines, respectively. The electron flow patterns above and below the plasma sheet are symmetric. Electrons move through the electron diffusion region, becoming accelerated by the reconnection electric field, and they are then expelled away from the X line as a super-Alfvénic jet.[23,24] The electron velocity distribution in region B is almost symmetric along, which leads to $P_{exy} \approx 0$. In regions A and C the symmetry is broken, which results in the non-zero values of P_{exy}.

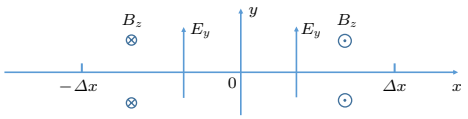

Fig. 4. The simplified configuration of electromagnetic fields in the vicinity of the X line for theoretical calculation.

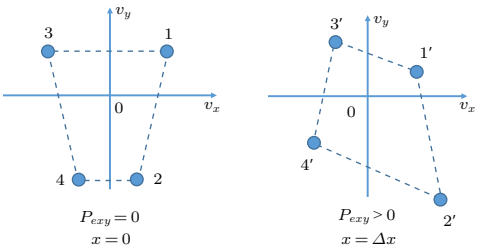

Fig. 5. The distributions of the four typical electrons in the (v_x, v_y) plane when they are located at $x = 0$ and $x = \Delta x$, respectively.

The balance between the reconnection electric field and the gradient of the electron pressure around in the electron diffusion region can be investigated by analyzing the typical electron trajectories.[25] Let us follow several electron motions along $z = 0$. First, we assume that the electromagnetic field is $\boldsymbol{E} = (0, E_y, 0)$ and $\boldsymbol{B} = (0, 0, B_z)$ in the electron diffusion region, as shown in Fig. 4. We consider the electron trajectories in the (v_x, v_y) plane of four typical electrons near the X line ($x = 0$). In Fig. 5, we plot the locations of these four electrons in the (v_x, v_y) plane when their positions are at $x = 0$ and $x = \Delta x$, respectively. Electrons 1 and 2 move from $x = 0$ to $x = \Delta x$, while electrons 3 and 4 move from $x = \Delta x$ to $x = 0$. The motions of the electrons can be described by Newton's equation

$$m_e d\boldsymbol{v}/dt = -e(\boldsymbol{E} + \boldsymbol{v} \times \boldsymbol{B}), \tag{5}$$

In our calculation, we assume that the velocities of electrons 1, 2, 3, and 4 at $x = 0$ are (a_1, b_1), (a_2, b_2), $(-a_1, b_1)$, and $(-a_2, b_2)$. Under this assumption, the velocities of electrons 1 and 2 at $x = \Delta x$ are

$$\begin{aligned} v'_{1x} &= a_1 - \frac{e}{m_e} b_1 B_z \Delta t \\ v'_{1y} &= b_1 - \frac{e}{m_e}(E_y - a_1 B_z)\Delta t \\ v'_{2x} &= a_2 - \frac{e}{m_e} b_2 B_z \Delta t \\ v'_{2y} &= b_2 - \frac{e}{m_e}(E_y - a_2 B_z)\Delta t, \end{aligned} \tag{6}$$

and the velocities of electrons 3 and 4 at $x = \Delta x$ are

$$\begin{aligned} v'_{3x} &= -a_1 + \frac{e}{m_e} b_1 B_z \Delta t \\ v'_{3y} &= b_1 + \frac{e}{m_e}(E_y + a_1 B_z)\Delta t \\ v'_{4x} &= -a_2 + \frac{e}{m_e} b_2 B_z \Delta t \\ v'_{4y} &= b_2 + \frac{e}{m_e}(E_y + a_2 B_z)\Delta t. \end{aligned} \tag{7}$$

Note that the time interval Δt is much smaller than the electron gyroperiod, we can then neglect $o(\Delta t^2)$ terms. Hence, the average velocities of these four electrons at $x = \Delta x$ are $\bar{v}'_x = 0$, $\bar{v}'_y = \frac{1}{2}(b_1 + b_2) + \frac{1}{2}\frac{e}{m_e} B_z \Delta t(a_1 + a_2)$. The contribution from these four electrons to the electron off-diagonal pressure tensor term P_{exy} can be calculated by

$$P_{exy} = m_e \sum_{j=1}^{4} (v'_{jx} - \bar{v}'_x)(v'_{jy} - \bar{v}'_y), \tag{8}$$

where the bar is the notation for an ensemble average. After substituting the velocity expressions of the electrons at $x = \Delta x$ (Eqs. (6) and (7)) into Eq. (8), we can obtain

$$\begin{aligned} P_{exy} = &-2(a_1 + a_2) e E_y \Delta t \\ &+ 2\frac{e^2}{m_e} B_z E_y (b_1 + b_2)\Delta t^2. \end{aligned} \tag{9}$$

Neglecting the $o(\Delta t^2)$ term, the result is

$$P_{exy} = -2(a_1 + a_2) e E_y \Delta t. \tag{10}$$

Hence, the gradient of the electron off-diagonal terms is

$$-\frac{1}{n_e e}(\nabla \cdot \boldsymbol{P}_e)_y = -\frac{1}{4e}\frac{P_{exy}}{\Delta x}. \tag{11}$$

After substituting the off-diagonal expression (10) at $x = \Delta x$ into Eq. (11) and using $\Delta x \sim (a_1 + a_2)\Delta t/2$, we can obtain

$$-\frac{1}{n_e e}(\nabla \cdot \boldsymbol{P}_e)_y = E_y. \tag{12}$$

This is the general Ohm law in the vicinity of the X line during the anti-parallel reconnection.

In summary, a 2D PIC simulation of anti-parallel magnetic reconnection has first been performed to

show that in the electron diffusion region the reconnection electric field is mainly balanced by the gradient of the electron pressure. Then, by following typical electron trajectories in the electromagnetic field, we also find that the resulted gradient of the electron pressure is equal to the reconnection electric field. The microphysical evidence, of which the reconnection electric field is mainly balanced by the gradient of the electron pressure in the electron diffusion region, is given.

References

[1] Vasyliunas V M 1975 *Rev. Geophys.* **13** 303
[2] Biskamp D 2000 *Magnetic Reconnection in Plasmas* (Cambridge: Cambridge University Press)
[3] Priest E and Forbes T 2000 *Magnetic Reconnection: MHD Theory and Applications* (Cambridge: Cambridge University Press)
[4] Guo J, Lu Q M, Wang S and Fu X R 2005 *Chin. Phys. Lett.* **22** 409
[5] Fu X R, Lu Q M and Wang S 2006 *Phys. Plasmas* **13** 012309
[6] Huang C, Lu Q M and Wang S 2010 *Phys. Plasmas* **17** 072306
[7] Lu S, Lu Q M, Huang C and Wang S 2013 *Phys. Plasmas* **20** 061203
[8] Drake J F, Swisdak M, Che H and Shay M A 2006 *Nature* **443** 553
[9] Pritchett P L 2006 *Geophys. Res. Lett.* **33** L13104
[10] Wang R S, Lu Q M, Li X, Huang C and Wang S 2010 *J. Geophys. Res.* **115** A11201
[11] Hesse M, Neukirch T, Schindler K, Kuznetsova M and Zenitani S 2011 *Space Sci. Rev.* **160** 3
[12] Hesse M and Winske D 1994 *J. Geophys. Res.* **99** 11177
[13] Hesse M, Schindler K, Birn J and Kuznetsova M 1999 *Phys. Plasmas* **6** 1781
[14] Lu Q M, Wang R S, Xie J L, Huang C, Lu S and Wang S 2011 *Chin. Sci. Bull.* **56** 48
[15] Pritchett P L 2001 *J. Geophys. Res.* **106** 3783
[16] Lu Q M, Huang C, Xie J L, Wang R S, Wu M Y, Vaivads A and Wang S 2010 *J. Geophys. Res.* **115** A11208
[17] Lu S, Lu Q M, Cao Y, Huang C, Xie J L and Wang S 2011 *Chin. Sci. Bull.* **56** 48
[18] Lu Q M, Lu S, Huang C, Wu M Y and Wang S 2013 *Plasma Phys. Control. Fusion* **55** 085019
[19] Birn J and Priest E R 2007 *Reconnection of magnetic field: Magnetohydrodynamics and Collisionless Theory and Observations* (Cambridge: Cambridge University Press)
[20] Guo J, Lu Q M, Wang S, Wang Y M and Dou X K 2004 *Chin. Phys. Lett.* **21** 1306
[21] Zhang Z C, Lu Q M, D O N G Q Li, Lu S, Huang C, Wu M Y, Sheng Z M, Wang S, Zhang J et al 2013 *Chin. Phys. Lett.* **30** 045201
[22] Wang P R, Huang C, Lu Q M, Wang R S and Wang S 2013 *Chin. Phys. Lett.* **30** 125202
[23] Shay M A, Drake J F and Swisdak M 2007 *Phys. Rev. Lett.* **99** 155002
[24] Phan T D, Paschmann G, Twitty C, Mozer F S, Gosling J T, Eastwood J E, Oieroset M, Reme H and Lucek E 2007 *Geophys. Res. Lett.* **34** L14104
[25] Cai H J, Ding D Q and Lee L C 1994 *J. Geophys. Res.* **99** 35

Chinese Physics Letters

Volume 32 Number 4 April 2015

PHYSICS OF GASES, PLASMAS, AND ELECTRIC DISCHARGES

CONDENSED MATTER: STRUCTURE, MECHANICAL AND THERMAL PROPERTIES

CONDENSED MATTER: ELECTRONIC STRUCTURE, ELECTRICAL, MAGNETIC, AND OPTICAL PROPERTIES

CROSS-DISCIPLINARY PHYSICS AND RELATED AREAS OF SCIENCE AND TECHNOLOGY